science, engineering and health studies

Research Article

Science, Engineering and Health Studies
https://lio1.tci-thaijo.org/index.php/sehs
ISSN (Online): 2630-0087

Machine learning parameter optimization for water stress detection in Khasi mandarin orange using an electronic nose

Rajdeep Choudhury[1], Chayanika Sharma[2], Robert Kwehayo[2], Sudipta Hazarika[3], and Utpal Sarma[2]*

[1] Bharti School of Telecommunication Technology and Management, Indian Institute of Technology Delhi, New Delhi 110016, India
[2] Department of Instrumentation & USIC, Gauhati University, Guwahati 781014, India
[3] Department of Physics, Madhabdev University, Narayanpur 784164, India

***Corresponding author**:
Chayanika Sharma
chayanika114@gmail.com

Received: *20 September 2025*
Revised: *29 September 2025*
Accepted: *17 October 2025*
Published: *6 November 2026*

Citation:
Choudhury, R., Sharma, C., Kwehayo, R., Hazarika, S., & Sarma, U. (2026). Machine learning parameter optimization for water stress detection in Khasi mandarin orange using an electronic nose. Science, Engineering and Health Studies, 20, 26020003.

ABSTRACT

Water stress is a critical factor affecting crop yield and quality in agriculture. Timely detection and management of water stress can significantly enhance crop productivity and resource efficiency. This study employs a custom-designed E-nose system to distinguish between four stages of water stress in Khasi mandarin orange plants. The research underscores the significant potential of machine learning in addressing water stress within agricultural practices, emphasizing the crucial role of integrating advanced technologies like E-nose and machine learning to tackle agricultural challenges. The optimized machine learning parameters demonstrate improved performance, achieving 99% accuracy in detecting water stress, enabling timely and precise interventions for potential crop damage mitigation and water usage optimization.

Keywords: E-nose; water stress; machine learning; optimization

1. INTRODUCTION

Sustainability in agriculture relies heavily on the efficient use of water, along with enhanced irrigation strategies (Puglisi et al., 2019). To adapt to water stress, plants develop a variety of mechanisms, including reduced transpiration, increased water use efficiency, reduction in the plant's above-ground portion, decreased stomatal conductance values, altered leaf water potential, decreased CO_2 assimilation values, altered amino acid metabolism, altered carbohydrate metabolism, altered abscisic acid content, decreased osmotic potential, and altered root-to-shoot ratio. However, these stress responses are not usually observed simultaneously (Sampaio et al., 2021; Gomes et al., 2004).

In 1979, Fereres et al. (1979) proposed the use of a pressure chamber to measure the relationship between relative water content (RWC) and balance pressure for assessing drought in plants. However, a primary source of error in a pressure chamber arises from the failure to prevent water loss during leaf excision. Another method for detecting drought in plants is the Crop Water Stress

index (CWSI). Various techniques, such as Landsat imaging and monitoring plant canopy temperature, can be employed to measure CWSI. However, significant fluctuations in canopy temperature measurements among plants pose a challenge, especially in windy conditions exceeding $3mS^{-1}$ (Jamshidi et al., 2021). Several other techniques have been reported by researchers to determine water stress in plants, including laser-induced fluorescence (LIF) spectroscopy (Marcassa et al., 2006), the photochemical reflectance index (PRI) (Suárez et al., 2010), RWC, Total Phenolic Content (TPC), proline content measurement (Hussain et al., 2018), thermocouple psychrometers, leaf in situ hygrometers (Bennett, 1990), and more. However, the main drawbacks of these conventional methods for water stress detection are the need for a large laboratory setup and a skilled operator.

Water stress can induce changes in the volatile organic compounds (VOCs) released by leaves. There are various techniques available for assessing leaf-emitted VOCs such as gas chromatography–mass spectrometry (GC–MS) and gas chromatography-flame ionization detector (GC–FID). Both GC–MS and GC–FID employ gas chromatography to separate the VOC blend, and detectors like mass spectrometry (MS), flame ionization detector (FID), biosensors, etc., can be used for identifying and quantifying the separated VOCs (Jansen et al., 2011). However, these techniques involve multiple steps, including VOC collection, sample preparation, separation, and quantification. Consequently, these processes can be time-consuming and require skilled operators (Ghaffari et al., 2010).

A simpler, yet very effective, method for determining water stress in plants is the use of electronic nose (E-nose) systems for monitoring leaf-emitted VOCs. That method doesn't require a large laboratory setup and a skilled operator, and has become widespread in industries related to agriculture and vegetation. E-nose devices are highly valued for their ability to identify specific gas mixtures released during various processes, making them essential tools in these industries (Wilson, 2013; Sharma et al., 2023a). The E-nose system is characterized by its speed, reliability, robustness, and portability. It typically comprises a sample collecting unit, a sensor array for VOC profiling, and a data acquisition unit for transferring data to a computational or storage device. The computational device, equipped with a suitable pattern recognition algorithm, then identifies and classifies the dataset (Shi et al., 2018). Consequently, an E-nose system proves effective in discriminating between stressed and non-stressed samples (Abbey et al., 2003).

The significance of machine learning in E-Nose systems lies in its ability to enhance odor recognition and classification. Machine learning enables E-Nose systems to learn from data and improve their performance over time. Machine learning includes data preprocessing to handle noisy and incomplete data, and feature extraction to derive relevant features from raw sensor data. This reduces the need for manual feature engineering and increases the system's efficiency (Sharma et al., 2023b; Ye et al., 2021; Gonzalez Viejo et al., 2021).

In the current study, a custom-designed E-nose system (Choudhury et al., 2019; Hazarika et al., 2020) is employed to discriminate among four different stages of water stress in Khasi mandarin orange plants.

The description of the system is provided in the following section. The dataset obtained from the experiments is fed into a computational device for optimization. Subsequently, various machine learning methods are compared for the classification of the dataset.

2. MATERIALS AND METHODS

2.1 Description of the prototype

A prototype E-nose system (Choudhury et al., 2019; Hazarika et al., 2020) was used in this work to monitor the water stress induced in Khasi mandarin orange plants. The block diagram & the complete experimental setup of the system are shown in Figure 1 and Figure 2, respectively. As depicted in Figure 2, the sample holder for the system is positioned on the top side of the sensor chamber. An airtight chamber, measuring 31 cm × 32 cm × 25 cm, was utilized to house an array of gas sensors (as detailed in Figure 4 and Table 1). Citrus fruits, including Khasi mandarin, are known to emit a range of VOCs such as ethanol, limonene, α-pinene, myrcene, and other terpenes and aldehydes, which contribute to their aroma profile. They can also be used as indicatives of fruit ripeness, stress, or spoilage. Among the selected sensors, TGS 2602, TGS 2620, MQ4, and MQ3 are particularly relevant, as they are sensitive to ethanol, methane, hydrogen, and toluene, which are the compounds commonly present in the VOC emissions of citrus fruits. In Figure 3[a], the inlet and outlet of the chamber are positioned on its front and back faces, respectively. To ensure uniform airflow throughout the chamber, two air showers with identical structures and dimensions were placed at the inlet and outlet sides within the chamber. Each hole in the shower had a diameter of approximately 2 mm, and consecutive holes were spaced 1 cm apart from each other.

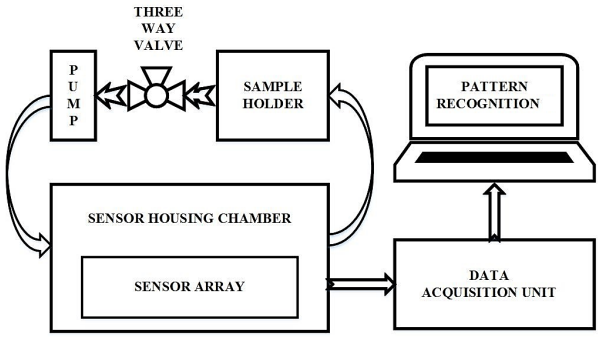


Figure 1. Block diagram of the E-nose system

The inlet and outlet of the pump were connected to the outlet of the sensor chamber and the inlet of the sample holder, respectively. Subsequently, the outlet of the sample holder was connected to the inlet of the chamber to facilitate the flow of odors emitted by the leaf samples, which were placed inside the sample holder, into the gas chamber.

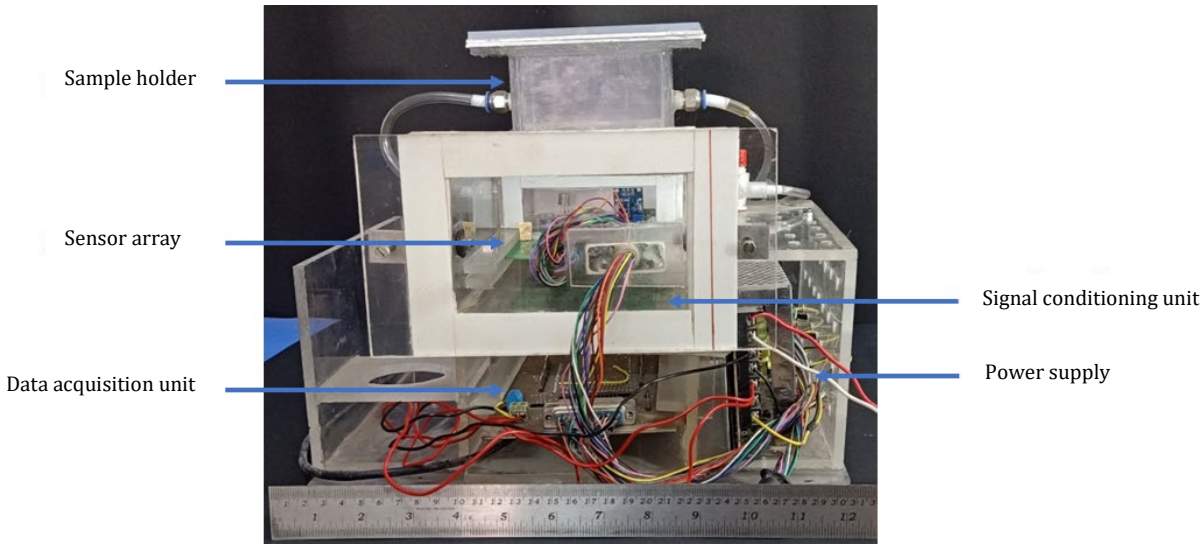


Figure 2. The complete E-nose setup

One of the most crucial components of an E-nose system is the data acquisition system (DAQ). The DAQ includes an analog-to-digital converter (ADC) with a 10-bit resolution and an 8-bit Atmel ATmega2560 microcontroller. The resistances of the electrochemical sensing layers of the gas sensors varies when odors enter the airtight chamber. These changes in resistance values on the sensor surface were recorded by converting them into equivalent voltages using potential divider circuits. The circuit diagram, taken from the sensors' datasheet, is illustrated in Figure 3[b]. These output voltage values were sent to a computing unit using the DAQ.

After each experiment, a three-way valve was employed to purge the sensor chamber by enabling the flow of fresh air inside. This valve was positioned between the sample holder and the air pump.

Table 1. The gas sensors used in the electronic nose system

Sensor name	Target gases	Type
TGS 2610	Ethanol, hydrogen, methane, propane, and iso- butane	MOS
TGS 2602	Ammonia, hydrogen sulphide, ethanol, and toluene	MOS
TGS 822	Methane, iso-butane, benzene, n-hexane, ethanol, carbon monoxide, and acetone	MOS
TGS 2444	Ammonia	MOS
TGS 2620	Methane, carbon monoxide, hydrogen, iso- butane, and ethanol	MOS
TGS 5141	Carbon monoxide	Electrochemical
MQ4	High sensitivity towards CH4 and natural gas. Less sensitive to alcohol and smoke	MOS
MQ3	High sensitivity towards alcohol and less sensitive to benzene	MOS
MQ6	LPG, iso-butane, and propane	MOS

2.2 Sample preparation & data collection

Orange trees were cultivated in a greenhouse at Gauhati University, India. For the experiments, 16 healthy Khasi mandarin orange plants of the same age group were selected. The greenhouse maintained constant parameters such as humidity, temperature, and light exposure, and the plants were observed for a period of 30 days.

To ensure optimal watering, a drip irrigation system was implemented in the greenhouse (Figure 5). This system delivered the appropriate amount of water to the plants at the right times. In a previous study (Choudhury et al., 2019), a method for calculating the required water quantity for plants was presented. The optimum water amount (W_0) was determined to be 162.85 mL/day. The equations to calculate reference evapotranspiration (ET_0) are given in Equation (1).

$$ET_0 = \frac{0.408\,\Delta\,(Rn_0 - G_h) + \gamma \frac{900}{T_0+273} V_2 (e_{s0} - e_{a0})}{\Delta + \gamma\,(1+0.34V_2)} \quad (1)$$

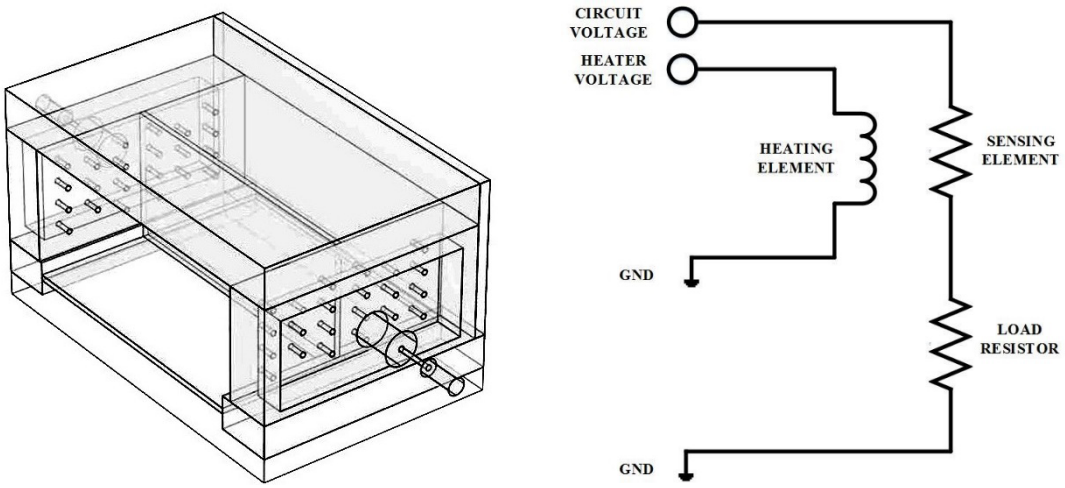
The crop evapotranspiration (ET_c) can be calculated as:

$$ET_c = K_{C0}\,ET_0 \quad (2)$$

The parameters used in the equations are described in Table 2.

Table 2. The parameters used in Equation (1) and Equation (2)

Parameters	Description	Unit
G_h	Heat flux density	$[MJm^{-2}day^{-1}]$
Rn_0	Crop surface's net radiation	$[MJm^{-2}day^{-1}]$
T_0	Daily mean temperature at a height of 2m	$[^0C]$
V_2	Wind speed at a height of 2m	$[ms^{-1}]$
e_{a0}	Actual vapor pressure	[kPa]
e_{s0}	Saturation vapor pressure	[kPa]
Δ	Slope of the vapor pressure curve	$[kPa^0C^{-1}]$
γ	Psychrometric constant	$[^0C^{-1}kPa]$
K_{c0}	Crop coefficient	



[a] [b]

Figure 3. [a] Sensor housing chamber; [b] schematic of the potential divider circuit

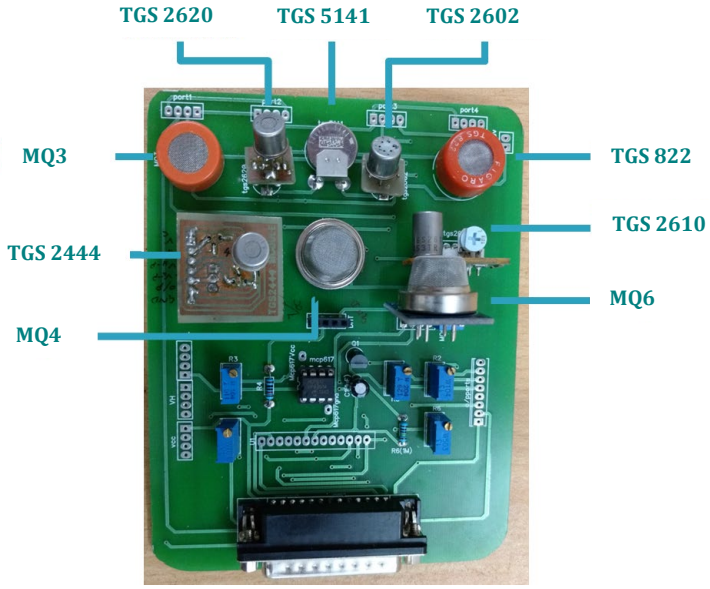


Figure 4. Gas sensors used in the system

The sample plants were categorized into four groups: CAT-I, CAT-II, CAT-III, and CAT-IV. The experimentation spanned a 15-day timeframe. Throughout the experiment, CAT-I plants received a consistent amount of irrigation water. On the first, fifth, and ninth days, watering of CAT-II, CAT-III, and CAT-IV plants was suspended.

For the experimental work, 10 g of fully grown sample leaves were collected on the fifteenth day. The excised leaves were then placed in the sample holder, and the air was circulated between the sample holder and the sensor housing chamber using the pump.

The sensor array's response was recorded and transmitted to the computational device using the DAQ.



Figure 5. Irrigation scheduling inside the greenhouse

2.3 Data collection protocol

The protocol followed by the E-nose system during the testing of samples is illustrated in Figure 6. The process starts with initializing connections between the computer and sensors to establish communication. After setup, the system checks if the sensors are ready to provide readings. If not, it loops back to ensure all sensors are operational before proceeding.

Once ready, the system takes readings from an array of 8 sensors. This data is transmitted to the computer for pattern recognition. The system then waits for 1 s to allow sufficient time for data transmission. Finally, the process repeats 300 times to gather enough data for analysis.

2.4 Pattern recognition using machine learning algorithms

To classify the dataset, various machine learning parameters were optimized in this study. Combinations of LDA and PCA algorithms with different machine-learning models were presented. For optimization purposes, the hyperparameters of the models were also tuned. Before classification, the entire dataset was divided into 80:20 train-test sets. Specifically, 80% (1176 samples) of the data was utilized for training, and the remaining 20% (294 samples) was reserved for the validation of the model's performance.

In prediction problems, preprocessing and optimization steps improve model performance on known (training) datasets. However, the model may perform poorly on unknown datasets. CV can address this by assessing model performance on unseen data. Among CV methods, K-fold CV is commonly used. In this technique, the dataset is divided into 'k' groups. As shown in Figure 7, with a 5-fold CV, the model was trained on four subsets and tested on the fifth, repeating this process five times.

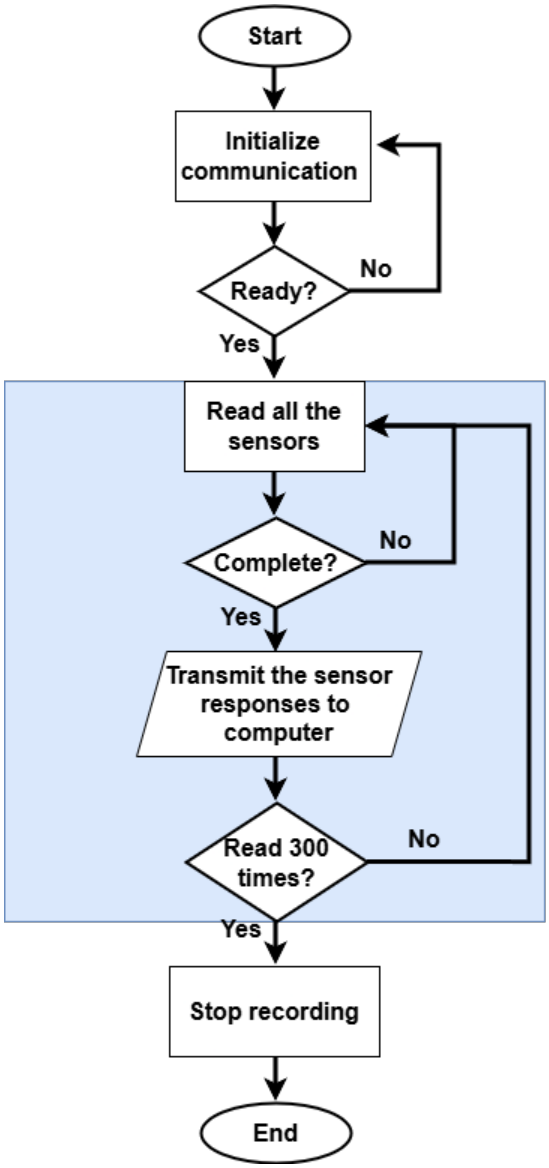


Figure 6. Protocol followed for sample testing

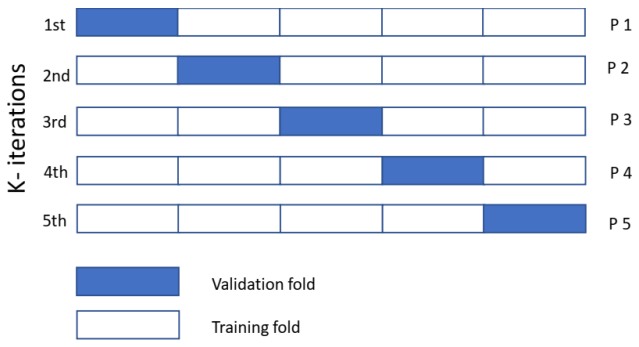


Figure 7. Pictorial representation of 5-fold CV

The ideal sensing system should feature a sensor array with the smallest number of sensors and maximum accuracy simultaneously. The dataset, obtained for four different stress levels from the system, was optimized using a radar/spider plot. The optimal number of sensors was determined by assessing each sensor's ability to discriminate among the samples.

A radar plot features multiple concentric circles, each representing a variable in a similar state. This type of chart is used to visualize multivariate data by plotting one observation along each axis and then connecting the data points to form a polygon (Sharma et al., 2022). The spread of the colored lines indicates the sensors' discriminant capacity, with a wider spread denoting higher discriminant ability.

3. RESULTS AND DISCUSSION

The obtained datasets were stored in a computational unit for analysis and classification. The radar plot for the sensing system is depicted in Figure 8. Following optimization, the four gas sensors that provided the most information regarding classification were selected: TGS 2602, TGS 2620, MQ4, and MQ3. While the radar plot (Figure 8) visually guided the selection of the most discriminative sensors, validation was performed to justify the exclusion of less informative sensors. Using all sensors, the classifiers achieved an average accuracy of 95% using LDA, whereas using only the sensors having the highest discriminative ability, the accuracy slightly improved to 95.91% with the same model, showing no performance loss despite reducing the sensor count. These numerical results clearly demonstrate that excluding lower-contributing sensors not only reduced the dimensionality of the dataset but also enhanced classification performance. The LDA plot for the optimized dataset using the radar plot is provided in Figure 9.

The sensor array is further optimized using PCA and LDA. The main benefit of PCA and LDA is that they simplify the data by converting many related variables into fewer uncorrelated and independent components while preserving as much original information as possible through different combinations. Furthermore, since LDA and PCA are dimension-reduction techniques, they help normalize the dataset and remove low-variance or redundant dimensions. In this study, we selected the top three components from each method to further classify the dataset, ensuring that the most discriminative information was retained for classification. The complete dataset and the datasets optimized using LDA and PCA were utilized as features for classification algorithms, including a bootstrap ensemble of k-nearest neighbors (KNN), support vector machines (SVM) with a radial basis function (RBF) kernel, decision tree (DT) classifier with bagging, and a random forest classifier (RFC). During the classification tasks, the previously mentioned 5-fold cross-validation technique was used to assess the robustness of the suggested models. The variation across the five folds was carefully evaluated. All classifiers, especially RF and DT, demonstrated consistently high accuracies (≥95%) regardless of the dimensionality reduction approach (radar plot, PCA, or LDA). This stability across distinct subsets and feature selection methods indirectly validates the generalization strength of the trained models. Furthermore, care was taken during the model development to avoid overfitting, including the shuffling of data before splitting and tuning the hyperparameters.

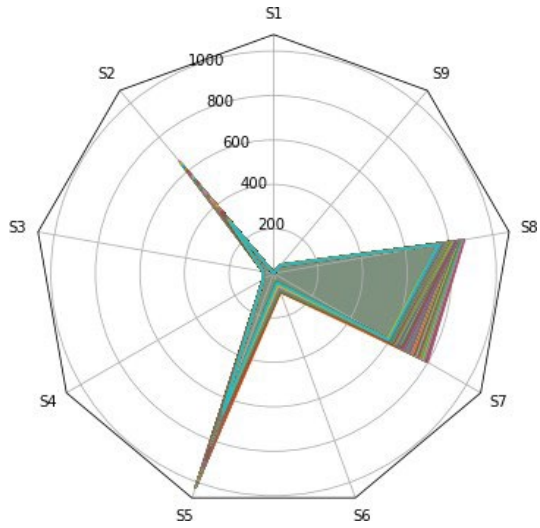


Figure 8. Radar plot obtained from the sensor responses

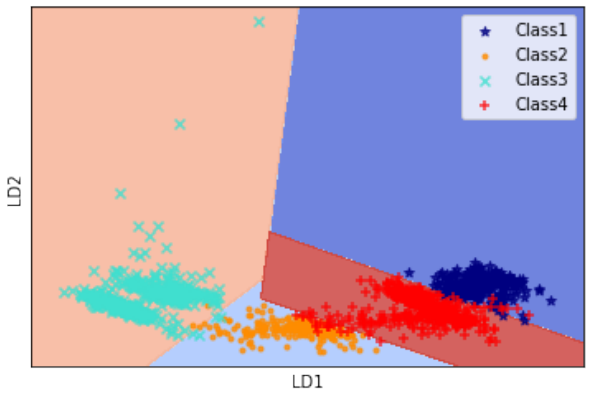


Figure 9. LDA plot obtained from the optimized dataset using radar plot

Table 3. Performance and prediction matrix of the system for the complete dataset and the dataset with LDA optimization

Classifier	Complete sensor array		Optimized sensor array using LDA	
	Accuracy	Confusion matrix	Accuracy	Confusion matrix
KNN	91%	[[37 0 0 8] [0 53 2 2] [0 2 95 0] [4 8 0 83]]	96%	[[40 0 1 1] [0 57 0 0] [0 0 97 0] [2 8 0 85]]
SVM	90%	[[34 0 0 11] [0 55 2 0] [0 2 95 0] [4 9 0 82]]	96%	[[43 0 0 2] [0 57 0 0] [0 0 97 0] [2 9 0 84]]
DT	92%	[[140 1 0 1] [4 77 0 0] [0 0 140 0] [0 0 0 78]]	95%	[[40 0 0 3] [0 54 0 3] [0 0 95 2] [4 4 0 87]]
RFC	95%	[[41 0 0 4] [0 55 0 2] [0 0 96 1] [1 8 0 86]]	96%	[[41 0 0 4] [0 55 0 2] [0 0 96 1] [1 3 0 91]]

Table 4. Performance and prediction matrix of the system with dataset after radar plotting and the dataset with PCA optimization

Classifier	Optimized sensor array using radar plot		Optimized sensor array using PCA	
	Accuracy	Confusion matrix	Accuracy	Confusion matrix
KNN	96%	[[43 0 0 2] [0 57 0 0] [0 0 97 0] [3 9 0 83]]	98%	[[45 0 0 0] [0 57 0 0] [0 0 97 0] [3 2 0 90]]
SVM	95%	[[45 0 0 0] [0 57 0 0] [0 2 95 0] [0 1 0 94]]	96%	[[45 0 0 0] [0 57 0 0] [0 0 97 0] [2 9 0 84]]
DT	97%	[[43 0 0 2] [0 55 0 2] [0 1 96 0] [0 3 0 92]]	**99%**	[[45 0 0 0] [0 57 0 0] [0 2 95 0] [0 1 0 94]]
RFC	98%	[[43 0 0 2] [0 57 0 0] [0 1 96 0] [1 3 0 91]]	**99%**	[[45 0 0 0] [0 57 0 0] [0 2 95 0] [0 1 0 95]]

For the classification using the KNN algorithm, the number of nearest neighbors was optimized for each case and chosen as 5, 7, 5, and 6 for the complete dataset and the datasets optimized using radar plotting, PCA, and LDA, respectively. In the RFC, the number of estimators was set to 100, and Gini was used as the criterion for evaluating the quality of a split. The performances of the sensor array with and without optimization for each classifier were compared and are presented in Table 3 and Table 4. The maximum accuracy of 99% was obtained using the DT classifier with bagging and RFC with PCA optimization.

4. CONCLUSION

In this study, the researchers demonstrated the significant potential of machine learning in addressing water stress in agricultural practices. By employing an E-nose system and leveraging machine learning algorithms, the findings reveal the importance of integrating advanced technologies like E-nose and machine learning to tackle agricultural challenges. Compared to the other studies, the optimized machine learning parameters showcased improved performance, achieving 99% accuracy in detecting water stress, which can lead to timely and precise interventions to mitigate potential crop damage and optimize water usage.

Moreover, the research will help in future advancements in precision agriculture, where E-nose systems combined with machine learning techniques can play a critical role in optimizing crop management and ensuring sustainable agricultural practices. As water scarcity and environmental concerns continue to rise in, the insights obtained from this study hold promise for enhancing agricultural productivity and flexibility in facing the changes of climatic conditions.

ACKNOWLEDGMENTS

The authors acknowledge the Department of Science & Technology, Govt. of India for providing financial assistance as the DST-Inspire fellowship program. The authors also acknowledge the Department of Biotechnology, Gauhati university for providing the green house.

AUTHOR CONTRIBUTIONS

U.S. and R.C. conceived the presented idea. R.C. and S.H. designed and developed the system and designed the methodology. R.C. and C.S. were involved in data collection and experimental work. C.S. and R.K. did the data analysis. The original draft was written by R.K. and C.S. Review and editing were done by U.S., R.C., and S.H. All authors discussed the results and contributed to the final manuscript.

REFERENCES

Abbey, L., Joyce, D. C., Aked, J., & Smith, B. (2003). Electronic nose-based discrimination among spring onions grown on two different soils at three water-deficit stress levels. *Acta Horticulturae*, *600*, 479–484. https://doi.org/10.17660/ActaHortic.2003.600.71

Bennett, J. M. (1990). Problems associated with measuring plant water status. *HortScience*, *25*(12), 1551–1554. https://doi.org/10.21273/HORTSCI.25.12.1551

Choudhury, R., Hazarika, S., & Sarma, U. (2019). Detection of water stress in Khasi mandarin orange plants from volatile organic compound emission profile implementing electronic nose. *International Journal of Engineering and Advanced Technology*, *9*(1), 133–137. https://doi.org/10.35940/ijeat.A1086.109119

Fereres, E., Cruz-Romero, G., Hoffman, G. J., & Rawlins, S. L. (1979). Recovery of orange trees following severe water stress. *Journal of Applied Ecology*, *16*(3), 833–842. https://doi.org/10.2307/2402857

Ghaffari, R., Zhang, F., Iliescu, D., Hines, E., Leeson, M., Napier, R., & Clarkson, J. (2010, July 18–23). *Early detection of diseases in tomato crops: An electronic nose and intelligent systems approach* [Conference session]. The 2010 International Joint Conference on Neural Networks (IJCNN), Barcelona, Spain. https://doi.org/10.1109/IJCNN.2010.5596535

Gomes, M. D. M. D. A., Lagôa, A. M. M. A., Medina, C. L., Machado, E. C., & Machado, M. A. (2004). Interactions between leaf water potential, stomatal conductance and abscisic acid content of orange trees submitted to drought stress. *Brazilian Journal of Plant Physiology*, *16*(3), 155–161. https://doi.org/10.1590/S1677-04202004000300005

Gonzalez Viejo, C., Tongson, E., & Fuentes, S. (2021). Integrating a low-cost electronic nose and machine learning modelling to assess coffee aroma profile and intensity. *Sensors*, *21*(6), Article 2016. https://doi.org/10.3390/s21062016

Hazarika, S., Choudhury, R., Montazer, B., Medhi, S., Goswami, M. P., & Sarma, U. (2020). Detection of Citrus Tristeza Virus in mandarin orange using a custom-developed electronic nose system. *IEEE Transactions on Instrumentation and Measurement*, *69*(11), 9010–9018. https://doi.org/10.1109/TIM.2020.2997064

Hussain, S., Khalid, M. F., Saqib, M., Ahmad, S., Zafar, W., Rao, M. J., Morillon, R., & Anjum, M. A. (2018). Drought tolerance in citrus rootstocks is associated with better antioxidant defense mechanism. *Acta Physiologiae Plantarum*, *40*(8), Article 135. https://doi.org/10.1007/s11738-018-2710-z

Jamshidi, S., Zand-Parsa, S., & Niyogi, D. (2021). Assessing crop water stress index of citrus using in-situ measurements, Landsat, and Sentinel-2 data. *International Journal of Remote Sensing*, *42*(5), 1893–1916. https://doi.org/10.1080/01431161.2020.1846224

Jansen, R. M. C., Wildt, J., Kappers, I. F., Bouwmeester, H. J., Hofstee, J. W., & van Henten, E. J. (2011). Detection of diseased plants by analysis of volatile organic compound emission. *Annual Review of Phytopathology*, *49*, 157–174. https://doi.org/10.1146/annurev-phyto-072910-095227

Marcassa, L. G., Gasparoto, M. C. G., Belasque, J., Lins, E. C., Dias Nunes, F., & Bagnato, V. S. (2006). Fluorescence spectroscopy applied to orange trees. *Laser Physics*, *16*, 884–888. https://doi.org/10.1134/S1054660X06050215

Puglisi, I., Nicolosi, E., Vanella, D., Lo Piero, A. R., Stagno, F., Saitta, D., Roccuzzo, G., Consoli, S., & Baglieri, A. (2019). Physiological and biochemical responses of orange trees to different deficit irrigation regimes. *Plants*, *8*(10), Article 423. https://doi.org/10.3390/plants8100423

Sampaio, A. H. R., Silva, R. O., Brito, R. B. F., dos Santos Soares Filho, W., da Silva Gesteira, A., Souza, L. D., & Coelho Filho, M. A. (2021). Sweet orange acclimatisation to water stress: A rootstock dependency. *Scientia Horticulturae*, *276*, Article 109727. https://doi.org/10.1016/j.scienta.2020.109727

Sharma, C., Barkataki, N., & Sarma, U. (2023b). A deep neural network with electronic nose for water stress prediction in Khasi mandarin orange plants. *Measurement Science and Technology*, *34*(12), Article 125152. https://doi.org/10.1088/1361-6501/acf8e3

Sharma, C., Choudhury, R., & Sarma, U. (2022). Sensor array optimization to design and develop an electronic nose system for the detection of water stress in Khasi mandarin orange. *Journal of Circuits, Systems and Computers*, *31*(9), Article 2250172. https://doi.org/10.1142/S0218126622501729

Sharma, C., Dey, A., Khatun, H., Das, J., & Sarma, U. (2023a). Design and development of a gas sensor array to detect salinity stress in Khasi mandarin orange plants. *IEEE Transactions on Instrumentation and Measurement*, *72*, Article 2006409. https://doi.org/10.1109/TIM.2023.3300476

Shi, H., Zhang, M., & Adhikari, B. (2018). Advances of electronic nose and its application in fresh foods: A review. *Critical Reviews in Food Science and Nutrition*, *58*(16), 2700–2710. https://doi.org/10.1080/10408398.2017.1327419

Suárez, L., Zarco-Tejada, P. J., González-Dugo, V., Berni, J. A. J., Sagardoy, R., Morales, F., & Fereres, E. (2010). Detecting water stress effects on fruit quality in orchards with time-series PRI airborne imagery. *Remote Sensing of Environment*, *114*(2), 286–298. https://doi.org/10.1016/j.rse.2009.09.006

Wilson, A. D. (2013). Diverse applications of electronic-nose technologies in agriculture and forestry. *Sensors*, *13*(2), 2295–2348. https://doi.org/10.3390/s130202295

Ye, Z., Liu, Y., & Li, Q. (2021). Recent progress in smart electronic nose technologies enabled with machine learning methods. *Sensors*, *21*(22), Article 7620. https://doi.org/10.3390/s21227620